Available online at www.sciencedirect.com

ScienceDirect

Procedia Manufacturing 34 (2019) 574–583

Procedia MANUFACTURING

www.elsevier.com/locate/procedia

47th SME North American Manufacturing Research Conference, Penn State Behrend Erie, Pennsylvania, 2019

Structural design optimization of knee replacement implants for Additive Manufacturing

Marinela Peto[a], Erick Ramírez-Cedillo[b,c], Adriana Hernández[d], Hector R. Siller[a*]

[a]*Department of Engineering Technology, University of North Texas. Denton Tx., 76207, United States of America*
[b]*Tecnológico de Monterrey, Av. Eugenio Garza Sada #2501 Sur, Monterrey, N.L. 64849, Mexico*
[c]*Laboratorio Nacional de Manufactura Aditiva y Digital (MADiT), México*
[d]*Hospital Universitario ''Dr. Jose´ E. González'', Monterrey, N.L., 64480, Mexico.*

* Corresponding author. Tel.: +1.940.565.2362. E-mail address: Hector.Siller@unt.edu

Abstract

Recent developments in additive manufacturing (AM) have led the way to extraordinary opportunities in the development and fabrication of surgical implants due to advantages that AM offers. The study of structural design optimization (SDO) involves strategies such as topology optimization (TO), shape optimization, and size optimization to achieve a desired functionality for a given set of loads and constraints while optimizing specific qualities such as the structure weight or uniform stress distribution. Thus, integration of structural design optimization (SDO) and additive manufacturing (AM) is a powerful way for designing and fabricating lightweight medical implants that replicate the biomechanical properties of the host bones, and minimize stress shielding related problems. This study is focused in proposing a setup of a proper methodology for the rapid development of optimized surgical implants. A tibia intramedullary implant for an 8-year old osteosarcoma patient is designed and optimized, through TO in Abaqus/Tosca, to reduce the weight of the implant and minimize stress shielding related problems. A weight reduction of about 30 % was achieved from structural design optimization. The overall viability of the proposed design concept was validated using finite element analysis (FEA), and a stainless steel 316 L prototype was fabricated via SLM. After analysing results, in order to address osseointegration it is proposed that lattice structures to be incorporated in future work. In addition to that, there will be structural modifications for the implant to be able to adjust as the patient grows.

Keywords: Knee arthroplasty; structural design optimization (SDO); topology optimization (TO); additive manufacturing (AM); stress shielding

1. Introduction

The human knee joint, which is the largest, most stressed and one of the most complex joint in the human body [1], consists of: femur, tibia, fibula, patella, cartilages, menisci, different ligaments and muscles. Knee arthroplasty is a surgical procedure that is used on diseased knee joints for diminishing pain or restoring function, and it can be performed as partial or total knee replacement [2]. The earliest model of knee implant, the Tibial Plateau Prosthesis, was developed in the late 1960s by MCKeever [3] and consisted of a single metal component. Further improvements of knee prosthesis have been effected by important findings such as the introduction of "high- density" polyethylene plastic as a bearing surface in 1963, the popularization of the use of methyl- methacrylate as a fixation grout in 1960, and the Federal Drug Administration's (FDA's)

10.1016/j.promfg.2019.06.222

approval of methyl methacrylate for general use in the United States in 1971 [4]. Since 1960 there was a continuous design evolution in total knee replacement satisfying new necessities [5] such as: anatomic congruence, articulacy, less material wear cost reduction, and better resistance to weight and stresses. Today, knee implants have characteristics such as [6]: increased mobility; multiple components; closer to natural knee geometry; reduced wear; different materials and coatings.

The most commonly used metallic biomaterials for bone fixation implants are [7,8]: stainless steel (ISO 5832-1), pure titanium (ISO 5832-2) and its alloys, and cobalt-chromium-based alloys (e.g. CoCrMo). These materials demonstrate an adequate combination of [7–9] bio-functionality (e.g. modulus of elasticity, strength, ductility, hardness and toughness) and biocompatibility (corrosion resistance and cytotoxicity of corrosion products). However, there are problems associated with the use of metallic implants [10,11] such as a possible release of metal ions, inflammatory reactions, possible toxicity, and problems related to stress shielding and bone loss.

Commercial metallic implants are five to six times stiffer than bone [10], and when an implant is inserted into a bone canal, the loads that before were carried by the bone only, will be shared between the implant and the bone. According to Wolff's law the bone adapts in accordance with mechanical stress acting upon it. If the loading on the bone increases, the bone will remodel itself over time increasing bone mass to become stronger, and vice versa [12]. Therefore, when an implant is introduced/fixed to the bone, the bone is subjected to reduced stresses resulting in significant problems associated with stress shielding [11] such as less dense and weaker bone. In addition to that, high stiffness of metallic implants may lead to cracking issues, loosening or failure of the implant [11]. Thus, a lot of work has been continuously done on materials, design optimization, and manufacturing processes to find adequate approaches to reduce or avoid stress shielding at the bone-implant interface. The stiffness of an implant results from material properties (modulus of elasticity) and its structural design (shape and dimensions) [8]. Attempts have been made to produce implants with similar stiffness as bone by using plastic or carbon enforced composites instead of metals. However, according to Richards and Perren [8]: implants with very low material stiffness do not as a rule offer an acceptable balance between biological and mechanical advantages. In many studies stress shielding phenomena is minimized by reducing the equivalent stiffness of metallic implants through the use of topology optimization (TO) [11], to create bone fixation designs with reduced material volumes.

Structural design optimization (SDO) methods provide the "best" values of system design and operating policy variables that will lead to the highest levels of system operating performance [13]. Topology optimization (TO), shape optimization, and size optimization are three broad categories of structural optimization, which focus on different aspects of the structure. TO can attain any shape within the design space, while shape and size optimization proceed with predefined configurations. Gradient-based or non-gradient-based mathematical techniques are used to achieve optimization. Today, there is a great interest in designing implants using topology optimization approach and producing them by AM techniques due its complex shape options of fabrication [7]. Thus, incorporating AM constraints into SDO techniques has drawn increasing attention [14] due to its promising benefits.

Topology optimization, which refers to the internal member configuration of a structure, is the most commonly used structural design optimization method. Since its introduction in 1988 in a seminal paper by Bendsøe and Kikuchi, TO has developed enormously in many different directions, and based on literature findings of the last 25 years, the most popular TO methods are: (a) Evolutionary based algorithms (EA), (b) Solid Isotropic Microstructure with Penalization (SIMP), (c) Evolutionary Structural Optimization (ESO), (d) Soft-Kill Option (SKO), and (e) Level-set methods (LSMs) [15,16]. In biomedical applications TO is used to improve implants [17]. The difficulty of solving an optimization problem is related to [18] the number of variables present and the mixture of the variables (discrete, continuous, Boolean). Therefore, the aid of computational tools become crucial in solving an optimization problem, which typically involves iteration. The assistance of finite element analysis is usually required to determine the satisfaction of constraints in problem solving. Commonly, topology optimized parts are too complex to be fabricated using conventional manufacturing methods. Additive manufacturing (AM) [19], which represents a class of manufacturing processes for fabricating parts from digital information by joining materials usually layer upon layer, provides great opportunity to fabricate designs that result from TO.

AM of biomaterials [9,20] is making significant progress towards numerous biomedical applications due to numerous advantages [21,22] that AM offers compared to conventional manufacturing such as the ease in which medical imaging data can be converted into solid objects; high customizability; ability to fabricate highly complex shapes; good dimensional accuracy; clean build environment; and less material used. Design for Additive Manufacturing (DfAM) [23] has been used to take full advantages of the unique capabilities from AM processes in creating optimally complex and efficient designs featuring intricate geometries, pores, and lattice structures. The powder bed fusion (PBF) processes are of particular interest, especially for fabrication of metallic medical devices [20]. For instance, selective laser melting (SLM) [24] and selective electron beam melting (SEBM) [25] have huge potential in orthopedic implants [26] and in direct customizable manufacturing of metallic cellular scaffolds. Fused deposition modeling (FDM) and stereolithography have found many applications in manufacturing of polymeric biomaterials. Also, due their cost advantages both processes have been used to produce biomodels. Bose et al. [20] presented a comprehensive review of AM techniques used for fabrication of different medical devices and medically relevant materials.

The main objective of this study is to assess a methodology for the improvement and optimization of customized medical implants in general. A case study is presented where the proposed procedure is applied to design, optimize, and fabricate a tibia intramedullary implant for an osteosarcoma patient. A schematic representation of the overall process followed for development of a customized tibia intramedullary implant is presented in Fig. 1 and explained forward.

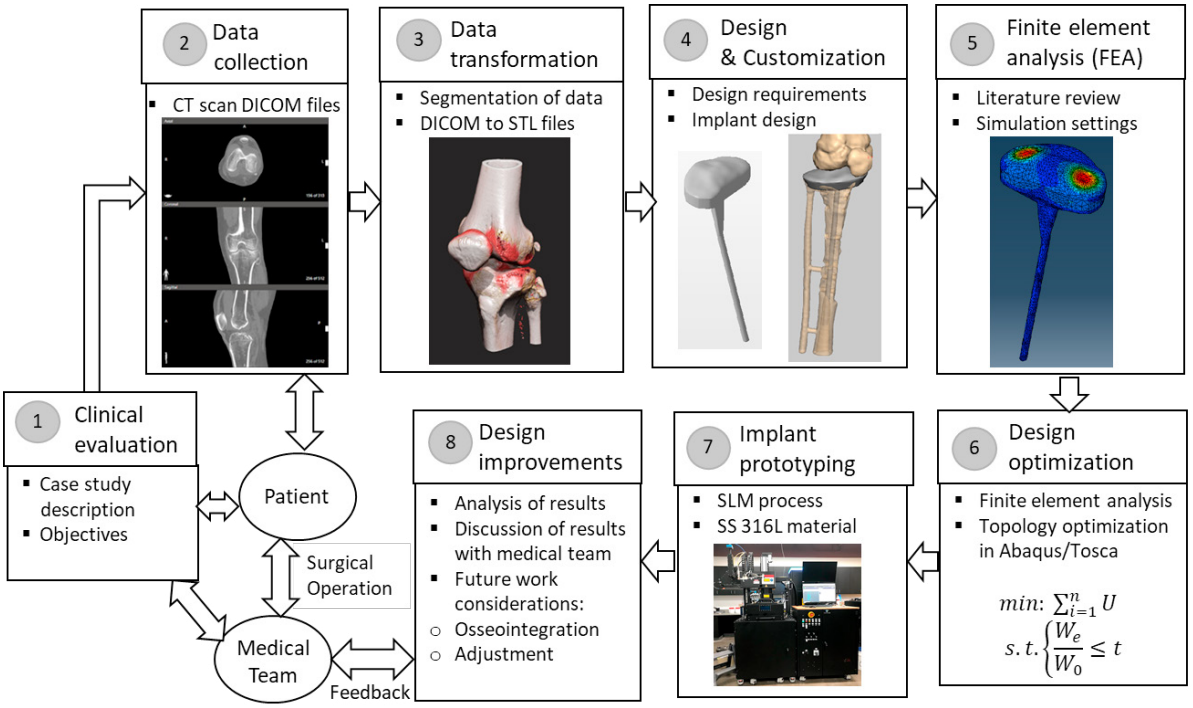

Fig. 1 Schematic of overall procedure for development of customized tibia intramedullary medical implant.

2. Materials and methods

The study was designated into five main stages which are: data preparation, customized design, structural optimization, prototype fabrication, and evaluation and future improvements. The data preparation phase involved CT scan data collection and data transformation. The transformation of data consisted of converting DICOM files into STL files, and furthermore STL files into IGES files. Evaluation phase incorporated virtual validation and frequent communication between medical team and engineering team. Finally, future design improvements were provided based on analysis of results and feedback from medical team. The next sections contain the explanation in more details of the entire processes and procedures used for this development.

2.1. Clinical evaluation

Case: An 8-year old child who is an osteosarcoma patient, had the tumor removed by surgical procedure from the right knee. Computed tomography (CT) scan and 3D joint images are presented in Fig. 2. The difference between the healthy knee and the diseased one is shown in Fig. 2, along with the original fixation plate. The weight of patient is 40 kg, and fixation method that will be used for the designed tibia intramedullary implant is press fit method.

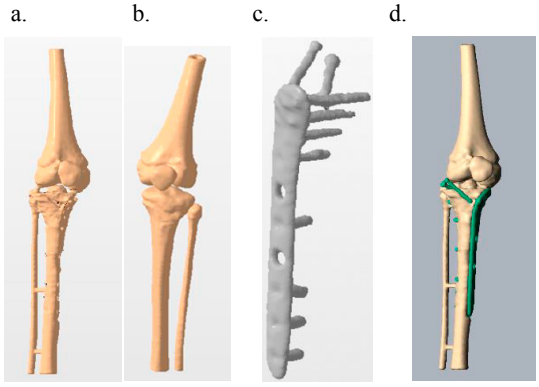

Fig. 2 STL images (not to scale) of (a) diseased right knee; (b) healthy left knee; (c) fixation plate; (d) original fixation assembly.

2.2. Imaging and scanning

After receiving a complete description about the case study and identifying objectives with medical team, data for the first step of the process chain for the tibia intramedullary implant design was collected from the patient through a CT scanner and processed as DICOM files (GE LightSpeed VCT 64 Slice CT). Since the design geometry of the implant is based on the CT scan of the healthy knee, the quality of the CT scan is crucial. Therefore, cuts of 1mm were performed to achieve accuracy on the STL.

2.3. Data transformation

After acquiring CT scan, the region of interest (tibia and femur bone) is identified and selected. The conversion of DICOM files into STL files is realized by means of a segmentation process using an open source software 3DSlicer 4.8 (Surgical Planning Lab, Harvard Medical School, Harvard University, Boston, USA).

2.4. Implant design and customization

The design requirements are identified based on three categories: (1) implant geometry; (2) implant fixation; (3) mechanical loads. The geometry of the designed implant is required to be as close as possible to the patient's tibia geometry. Therefore, the patient's healthy left knee files are used to construct the geometry of the implant in terms of mimicking the shape of the tibia. Modifications were made accordingly to the requirements from the medical team regarding dimensions and the capability of the designed implant to fit into the patient's bone. The implant was required to be bigger compared to the original tibia since the patient is a child and she will grow. The dimensions for height, width, and length of the implant are 152 mm, 62 mm, and 43 mm, respectively. The implant will be placed into the bone using press fit method by pushing the intramedullary stem inside the remaining bone and fastening with bone cement below the upper part of the implant. Geomagic Freeform [27] is used for sculpting and generating the initial biomodel design. Mechanical loadings applied in finite element analysis are defined based on literature review [28–33], and calculated accordingly for the body weight (BW) of the patient which is 40 kg.

2.5. Materials

Considering requirements of material properties used in surgical implants [9] such as biocompatibility, bulk properties and surface properties, it was decided to use stainless steel (SS) 316L for the simulation and fabrication of the part via selective laser melting (SLM) technology. Since stainless steel 316L is the most corrosion resistant when it comes in contact with biological fluid [34], it is commonly used in surgical procedures to replace biological tissue or to help stabilize a biological structure supporting the healing process [34]. The cortical-trabecular bone matrix material properties were selected based upon pre-existing published data [35]. Table 1 shows a summary of implemented material properties of the austenitic AISI SS 316 L [36] employed for simulation of the tibia intramedullary implant in Abaqus/CAE, and fabrication of the prototype. The chemical composition of SS316L used for SLM was Fe (Balance), Cr (17.5-18%), Ni (12.5-13.00%), Mo (2.25-2.50%), Mn (<2%), Si (<0.75%), Cu (<0.5%), N (<0.1%), O (<0.1%), P (0.025%), C (0.03%), S (0.01%) with an average particle size of 45±15 µm (LPW technology, Widness, UK). The mechanical properties of additively manufactured components using the austenitic AISI SS 316 L are shown in Table 2.

Table 1 Generic data – SS 316L-0407 wrought material [36].

	SS 316L-0407
Density [g/cm^3]	7.99
Thermal conductivity [W/mK]	15.6
Melting range [°C]	1,371-1,399
Coefficient of thermal expansion [K^{-1}]	16x10^{-6}
Poisson's Ratio	0.265

Table 2 Mechanical properties of additively manufactured components [36].

	As-Built Direction	
	Horizontal (XY)	Vertical (Z)
Upper tensile strength (UTS)	590 - 690 MPa	485 - 595 MPa
Yield strength	470 - 590 MPa	380 - 560 MPa
Elongation at break	25 - 55%	30 - 70%
Modulus of elasticity	197 GPa ± 4 GPa	190 GPa ± 10 GPa
Hardness (Vickers)	210 - 214 HV0.5	114 - 226 HV0.5

2.6. Finite element analysis

2.6.1. Biomechanics of knee joint

The biomechanics of the knee joint are highly complicated [28] due to complexity related to: structural and mechanical properties of bone, cartilage and other soft tissues; forces experienced by certain structures during different activities and displacements occurring across multiple planes of motion; contact pressures, and joint kinematics. Therefore, there are various modelling approaches [28–31] that have been used for computation of knee forces. The determination of knee forces has been studied by mathematical modeling [28] or direct measurements using instrumented knee prosthesis [30]. Inverse dynamics and forward dynamics are the most popular mathematical modelling approaches used to relate knee kinematics and external forces to internal joint contact forces [29]. Since the accurate modeling of the knee hinders due to many factors, there are significant differences in predictions of knee forces due to diversity of approaches, modeling assumptions, and algorithms used [29]. Several software packages, such as Abaqus, Comsol, LS-Dyna, ANSYS, etc. are used for simulation and analysis work as an important tool for understanding knee biomechanics.

Due to different daily life physical activities, the peak forces acting on the tibia plateau vary significantly [29]. Previous studies have found, from measuring forces in distal femur replacement and transforming to the knee joint, that during typical normal level walking a resultant joint reaction force is equivalent to approximately three times the body weight (BW) [29,33,35]. Kutzner et al. [37] determined loading of knee joint during activities of daily livings using in vivo measurements. According to their in vivo experiments it was reported that the average peak resultant forces in terms of body weight (BW) from the highest to the lowest are: stair descending (3.46 BW), stair ascending (3.16 BW), level walking (2.61 BW), one legged stance (2.59 BW), knee bending (2.53 BW), standing up (2.46 BW), sitting down (2.25BW) and two legged stance (1.07BW). Therefore, for most daily activities according to

Kutzner et al. the resultant forces fall typically in the range of 220 – 350% BW [37].

2.6.2. Simulation settings

Normal walking activity consists of two main phases: stance phase and the swing phase. During the normal gait cycle approximately 60% of the time is compromised by stance phase and 40% by the swing phase. Morrison [38] has shown that the maximum joint loading occurs during the stance phase only. There are six sub-phases in the stance phase which are: heel strike, foot flat, mid-stance, heel off, and toe off. The loading used in this paper is based on the work of Morrison [38] who used analytical musculo-skeletal models and gait data for calculation of the maximum mean tibio-femoral compressive force. According to Morrison [38], the maximum mean tibio-femoral compressive force was calculated to be about three times body weight (BW) at the stance phase during level walking. The heel-strike stance phase during normal gate is simulated, where no ligament loading is applied to the system, using a static analysis with a dynamic load magnification factor adopted from the work of Bautista [35]. Furthermore pressure is used instead of concentrated loads guided by the work of Müller-Karger et al. [39].

The correction of the STL file geometry and the conversion from STL files into IGES files was done using SolidWorks 2017 (Dassault Systèmes SolidWorks Corporation, Waltham, MA, USA).The IGES files were imported to Abaqus/CAE 2018 (Dassault Systèmes Simulia Corp, Johnston, RI, USA) for the finite element analysis. A loading with a magnitude of 1,177.2 N (three times the patient's body weight) is distributed between the medial and lateral condyles, as constant distributed force, approximately covering contact areas of 178.6 mm^2 and 159.5 mm^2, as shown in Fig. 3.

The encastre function is used for boundary condition in Abaqus/CAE 2018, simulating the situation where an assumed fully fixed condition exists [35]. This boundary condition function restricts the bottom faces and all the connecting nodes on it in three directions, preventing the displacement and rotation. A mesh with a total 80979 nodes and 55009 total number of quadratic tetrahedral elements of type C3D10, was used as shown in Fig. 3-a.

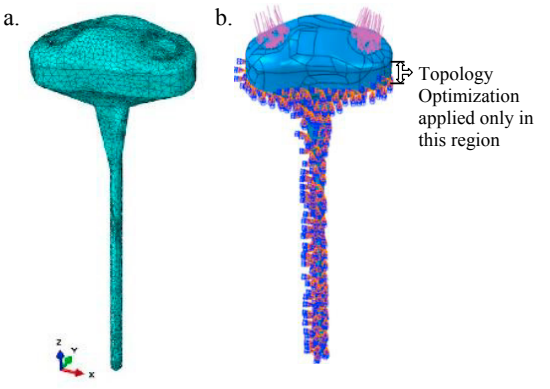

Fig. 3 (a) Meshed model of initial customized tibia intramedullary implant using C3D10 element type. (b) Loadings and boundary conditions applied on tibia intramedullary implant for FEA, and topology optimization work space.

2.7. Structural design optimization

2.7.1. Topology optimization using Solid Isotropic Material with Penalization (SIMP) approach

Topology optimization (TO) [13] of solid structures refers to the internal member configuration of a structure indicating the regions where holes will be located, the amount of the holes, their shapes, and the connectivity of the domain. TO is a mathematical method that determines the material placement in given domain to achieve a desired functionality for a given set of loads and constraints while optimizing for certain qualities such as minimal material usage or uniform stress distribution [23]. Guided by gradient computation or non-gradient algorithms TO builds on a repeated analysis and design update steps [40]. TO was introduced in 1988 in a seminal paper by Bendsøe and Kikuchi [41], and since then it has developed immensely in many different directions. General form of a TO problem to find the material distribution that minimizes an objective function **F**, subject to volume constraint $g_0 \leq 0$, and possibly other constraints $g_i \leq 0$, i = 1,…, n, can be written as [42]:

$$min: \quad \boldsymbol{F} = F(\boldsymbol{u}(\rho), \rho) = \int_0^{\varphi} f(\boldsymbol{u}(\rho), \rho) dV \tag{1}$$

$$subject\ to: \begin{cases} g_0(\rho) = \int_0^{\varphi} \rho dV - V_0 \leq 0 \\ g_j(\boldsymbol{u}(\rho), \rho) \leq 0 \quad with\ j = 1, \dots, n \\ \rho(\boldsymbol{x}) = 0\ or\ 1 \quad \forall\ x \in \varphi \end{cases} \tag{2}$$

The density variable $\rho(\mathbf{x})$ describes the material distribution, and it can be either 0 (void) or 1 (solid) in any point in the design domain φ. Linear or non-linear state equations are satisfied by the state field **u**. V represents the volume of the structure.

A widely used density-based TO approach is solid isotropic material with penalization (SIMP) [13,43,44] where the geometry is described via a material distribution which is typically discretized using element-wise invariable or nodal shape functions. SIMP is also known by different names such as density method, power law, or material interpolation. This method uses a "density" $\rho(x)$ of a finite element as only design variable for each element [45] . The design variable and is normalized to have a value between zero (void) and one (solid). The relation between the design function "density" $\rho(x)$ and properties of an isotropic material E^0_{ijkl} is given by power law as follows [13]:

$$E_{ijkl}(x) = \rho(x)^P \times E^0_{ijkl}, \qquad P > 1 \tag{3}$$

$$\int \rho(x) d\Psi \leq V\ ; \quad 0 \leq \rho(x) \leq 1, \quad x \in \psi \tag{4}$$

The density is interposed between material properties $E_{ijkl}(\rho = 0) = 0$ and $E_{ijkl}(\rho = 1) = E^0_{ijkl}$. The volume of the structure is evaluated as $\int \rho(x) d\Psi$, where: ψ is the reference domain. "P" is a penalty factor that is used to penalize design variables not equal to 0 or 1, and its value is increased gradually from unity and is usually between 2 and 4 [46]. Tamimi et al. [11] employed a topology optimization using the SIMP method with minimizing the strain energy (maximizing the stiffness), constraining the volume. Tamimi et al. found out [11] that even though the TO used intended to increase stiffness

of each element, due to high percentage of volume reduction it was observed that the lightweight effect contributes to decrease of the equivalent stiffness of the component resulting in reducing stress shielding phenomena. Therefore, based on the work of Tamimi et al. [11], it was decided to use an objective function that minimizes strain energy for the topology optimization of the tibia intramedullary implant under a weight constraint.

2.7.2. Computational design optimization process

The design optimization process is performed using topology optimization method in Abaqus/Tosca Structure 2018 (Dassault Systèmes Simulia Corp, Johnston, RI, USA), and the workflow of the computational design optimization is presented in Fig. 4.

The objective function used is to minimize design response values of strain energy. The density update strategy used in Abaqus is normal, and initial density used the optimization product default. The values of minimum density, maximum density, and maximum change per design cycle used were 0.001, 1, and 0.25 respectively. The convergence criteria to be fulfilled is 0.001 for objective function delta criterion and 0.005 for element density delta criterion. A penalty factor of 3 is used for material interpolation technique.

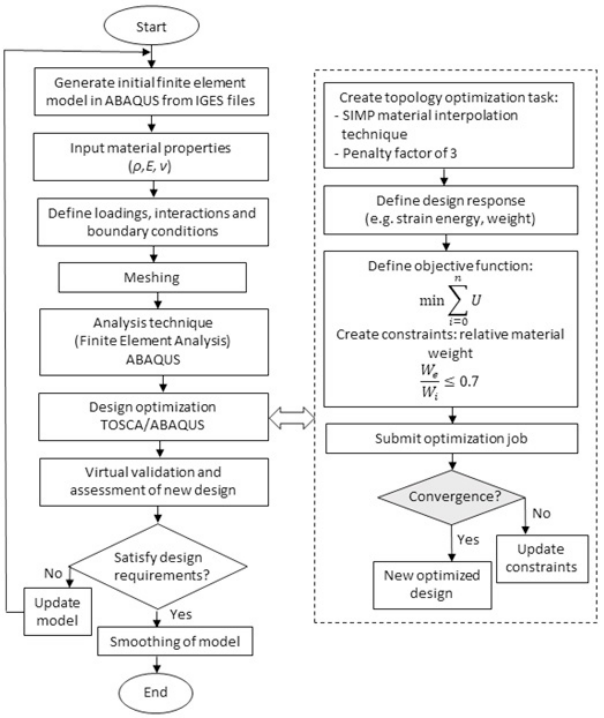

Fig. 4 Computational design optimization workflow using Abaqus/Tosca.

The weight constraint for a fraction of the initial value less or equal than 0.7 was used. This value was decided based on specified design requriements and topology optimizations attempts performed in Abaqus/Tosca. The stem of the implant is required to be solid and the geometry of the upper and bottom portions of the tibia to be kept the same as the original biomodel. Therefore, the workspace of the topology optimization was determined to be the middle portion of the tibia (Fig. 3), which is 145 grams comprehending 45% of the entire weight of the implant which is 321.6 grams. Several topology optimization attempts were performed starting with values of weight constraint for a fraction of the initial value greater than 0.56, until it was found that the value of 0.7 was optimal for achieving weight reduction and allowing for further improvements such as incorporating lattice structures in the next phase. Load regions and boundary condition regions were kept frozen in the topology optimization task.

2.8. Implant fabrication using Selective Laser Melting (SLM)

The intramedullary tibia implant was fabricated by SLM using an Aconity 3D MIDI (Aconity GmbH, Herzogenrath, Germany). This system has a laser beam source (CW fiber laser with a λ = 1070 nm) with a maximum power of 1000W and a diameter spot in a range of 80-500 μm, and it has a working volume of a cylinder of 170 mm and height of 150mm. Argon was used as an inert gas to reduce corrosion, avoid contamination, and oxidation of the powder with a flow of 7 L/min. Laser process parameters are shown in Table 3.

Table 3 Selective laser melting process parameters.

Laser parameter	Value
Laser Power [W]	170
Laser modulation frequency [MHz]	1
Laser modulation width [μs]	10,000
Laser off delay [μs]	5
Laser on delay [μs]	20
Beam spot [mm]	0.08
Scanning laser speed [mm/s]	500

The optimized implant was converted into STL and introduced into Netfabb Premium 2019 (Autodesk, California, USA) for the generation of the layers (CLI files) where a layer thickness of 50 μm was selected. The quad islands strategy was used as the laser scanning strategy with a quad height and width of 10 mm X 10 mm, a hatch distance of 0.12 mm, an initial and rotation angle per layer of 0º and 67º respectively and a translation layer of 0.001 mm. Quad islands strategy also named chessboard by other authors, and with a rotation angle between layers has been proved to have less presence of the residual stresses on the parts [47]. Even though roughness is higher [48] with this laser scanning strategy, the resulting topography can be suitable for the interaction between bones, and osteoblasts responded better in proliferation and adhesion with altered surfaces higher than 30 μm [49]. The support material was designed with solid lines with small unions with the platform and the implant for easy removal. Each one of the CLI files was compressed into an ILT file and introduced into Aconity Studio (Aconity 3D, Herzogenrath, Germany) for its fabrication.

3. Results and discussion

3.1. Initial customized tibia intramedullary implant

Following the procedure that was described in section 2.4, an initial biomodel of tibia intramedullary implant was designed. The front view and the side view of the designed implant are shown in Fig. 5-a and Fig. 5-b respectively. The dimensions for the customized designed tibia intramedullary implant are: 152 mm high, 62 mm wide, and 43 mm long. The weight of the customized biomodel using stainless steel 316L material is calculated to be 321.58 g.

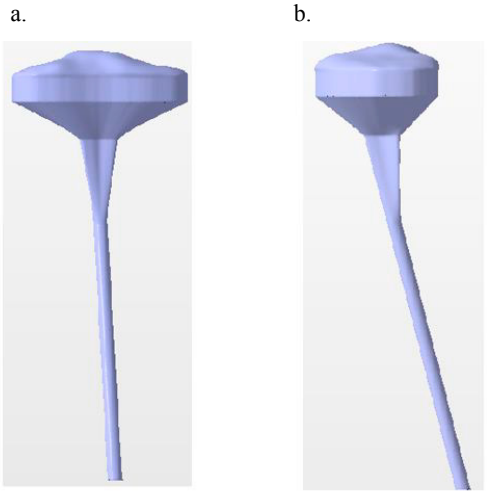

Fig. 5 Designed tibia intramedullary implant: (a) front view; (b) side view.

3.1.1. Finite element analysis initial customized tibia intramedullary implant

The finite element analysis (FEA) was performed in Abaqus using the loadings and boundary conditions defined in section 2.6. The results of finite element analysis for contour plots of displacement and von Mises stress are shown in

Fig. 6. From the displacement and Von Mises contour plots can be seen that the maximum magnitude of displacement is 1.643×10^{-4} mm and maximum Von Mises stress is 7.32 MPa.

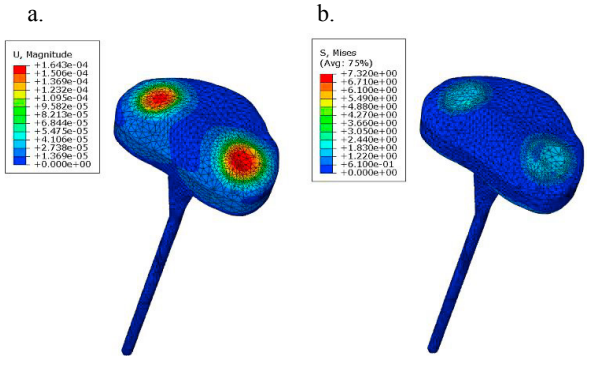

Fig. 6 Finite element analysis results before the optimization. (a) The displacement contour plot [mm]. (b) Von Misses contour plot [MPa].

3.2. Topology optimization results

TO was performed only for the top part (not for the stem), and the generated results are shown in Fig. 7. The weight of the implant is reduced by almost 30%, measuring a value of 225.38 g compared to initial weight of 321.58 g. This optimization sets the stage for further improvements that will be incorporated in the next phase, such as putting lattice structures in order to promote bone ingrowth and contribute to reduction of stress shielding problems. In addition to that, the implant will be post processed for further refinements.

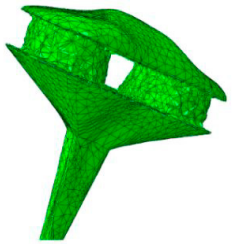

Fig. 7 Optimized tibia intramedullary implant.

3.2.1. Finite element analysis for optimized implant

The results of finite element analysis after the optimization are shown in Fig. 8, and as it can be seen from contour plots, the maximum magnitude of displacement is 1.879×10^{-4} mm and the maximum Von misses stress is 7.448 MPa.

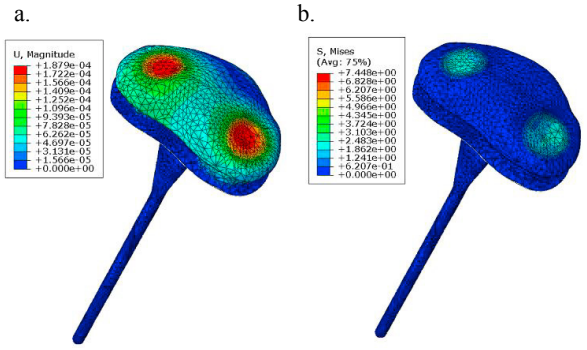

Fig. 8 Finite element analysis results after optimization. The displacement contour plot [mm] (left) and Von Misses contour plot [MPa] (right).

3.3. Comparison of FEA results for original and optimized tibia intramedullary implant

The comparison of finite element analysis results of original and the optimized model show not a significant change in the values of displacement and von Mises stress. The maximum magnitude of displacement increases from 1.643×10^{-4} mm for original model to 1.879×10^{-4} mm for the optimized model. Von Mises stress on the tibia intramedullary implant has also increased slightly from 7.32 MPa for original model to 7.448 MPa for optimized model. From the analysis and comparison of the results of FEA it can be stated that the topology optimization is beneficial for improvement of the implant by achieving a weight reduction of 30% while the maximum

magnitude of displacement and maximum von Mises stress increase only by 14.4% and 1.7 % respectively.

3.4. SLM processing for prototyping

The intramedullary implant was orientated lying to the platform to achieve a good surface topography in its interaction with the upper bone (femur). To start the process, the argon flow was controlled at the desired level and the chamber was pressurized with a total time of 45 minutes. During the SLM process, the powder was always well distributed over the platform with a platform offset of 0.05 mm and supply factor of 3 powder (3 times the layer thickness) without signs of warping on the edges of the implant, or over melted layers. The machine took 6 hours to produce the implant and 1 hour for the post-processing and cleaning. Figure 9 shows the resulted intramedullary tibia implant fabricated with SLM. The part has a bright metallic color, and it shows no defects on its surface or balling effect, no warping, or any deformation between the part and the building platform.

Also, in order to measure the surface roughness of the prototype fabricated via SLM, it was performed a surface characterization analysis with the aid of CHR 150, chromatic confocal sensor. Based on the conducted analysis, the value of surface roughness parameter Ra was found to be 9.63 µm.

Fig. 9 Stainless steel 316L optimized tibia intramedullary implant fabricated via selective laser melting process.

3.5. Future design improvements

Compared to structural design optimization methods, the replacement of solid volumes by lattice structures may also offer robust solutions to different multi objective problems that involve unsureness of loading conditions [11]. Due to their high strength to weight ratio, lattice structures used in orthopaedic implants are found to be very beneficial for bone ingrowth stimulation (osseointegration) and reduction of problems related to stress shielding phenomena [50]. Furthermore, the geometry of lattice structures can be modified to accomplish certain levels of required performance. TO have been used by many researchers as an effective method in designing optimized unit cells that lead to several structural and functional improvements of orthopedic implants.

Therefore, in order to further improve the designed tibia intramedullary implant, lattice structures will be considered in future work. The results of topology optimization are valuable in identifying the regions where the material is not critical and therefore can be removed from the model. The optimized model will be used as a guide in taking the decision of replacing solid volumes with lattice structures in order to generate lighter design, while offering bone ingrowth simulation with suitable level of stiffness and energy absorption under static and dynamic loading.

Also, since the patient is a child, structural design modifications will be considered in future work allowing for adjustments of the implant as the patient grows.

4. Conclusions

This study has proposed a methodology that can be used for improvement of customized medical implants in general. A knee prosthesis case study is presented where the proposed procedure is applied to design, optimize, and fabricate a tibia intramedullary implant for an 8-year old osteosarcoma patient. Customization is focused on matching the geometry of the implant as close as possible to the original anatomy of the patient's tibia. In order to further improve the designed implant, structural design optimization is considered. Through performing a computational topology optimization, it was achieved 30% weight reduction. The process chain was validated virtually using Abaqus/Tosca, and a proof of concept is shown by fabricating a stainless steel 316L prototype via selective laser melting (SLM) process.

Future considerations for further improvement of tibia intramedullary implant are proposed. Lattice structures will be incorporated in next steps of implant design to stimulate bone ingrowth and reduce stress shielding phenomena. Further structural modifications will be also considered for implant adjustments due to patient growth.

5. Acknowledgments

The research was possible with the support of the College of Engineering of the University of North Texas, the Conacyt Mixed Scholarships Program and the Research Group in Advanced Manufacturing of Tecnologico de Monterrey. The authors acknowledge also the support of Dr. Adrian Negreros from Hospital Universitario and Dr. Carlos Cuervo from Hospital Zambrano Hellion.

References

[1] N.K. Sahu, A.K. Kaviti, A Review of Use FEM Techniques in Modeling of Human Knee Joint, J. Biomimetics, Biomater. Biomed. Eng. 28 (2016) 14–25.

[2] S. Zanasi, Innovations in total knee replacement: New trends in operative treatment and changes in peri-operative management, Eur. Orthop. Traumatol. 2 (2011) 21–31.

[3] D.C. McKeever, J.C. Pickett, THE CLASSIC: Tibial

Plateau Prosthesis, Clin. Orthop. Relat. Res. 440 (2005) 4–8.
[4] R.P. Robinson, The early innovators of today's resurfacing condylar knees, J. Arthroplasty. 20 (2005) 2–26.
[5] A. Causero, P. Di Benedetto, A. Beltrame, R. Gisonni, V. Cainero, M. Pagano, Design evolution in total knee replacement: which is the future?, Acta Bio Medica Atenei Parm. 85 (2014) 5–19.
[6] B.C. Carr, T. Goswami, Knee implants - Review of models and biomechanics, Mater. Des. 30 (2009) 398–413.
[7] S.X. Xiaojian Wang Shiwei Zhou, Wei Xu, Martin Leary, Peter Choong, M. Qian, Milan Brandt, Yi Min Xie., Topological design and additive manufacturing of porous metals for bone scaffolds and orthopaedic implants: A review, Biomaterials. 83 (2016) 127–141.
[8] S.M.P. R. Geoff Richards, Implants and Materials in Fracture Fixation, J. Chem. Inf. Model. 53 (2013) 1689–1699.
[9] M. Saini, Implant biomaterials: A comprehensive review, World J. Clin. Cases. 3 (2015) 52.
[10] K.S. Katti, Biomaterials in total joint replacement, Colloids Surfaces B Biointerfaces. 39 (2004) 133–142.
[11] A.A. Al-Tamimi, C. Peach, P.R. Fernandes, A. Cseke, P.J.D.S. Bartolo, Topology Optimization to Reduce the Stress Shielding Effect for Orthopedic Applications, Procedia CIRP. 65 (2017) 202–206.
[12] M.I.Z. Ridzwan, S. Shuib, A.Y. Hassan, A.A. Shokri, M.N. Mohammad Ibrahim, Problem of stress shielding and improvement to the hip implant designs: A review, J. Med. Sci. 7 (2007) 460–467.
[13] M.P. Bendsøe, O. Sigmund, Topology optimization: theory, methods, and applications, Vasa. (2003) 370.
[14] Y. Wang, Z. Kang, ScienceDirect A level set method for shape and topology optimization of coated structures, Comput. Methods Appl. Mech. Engrg. 329 (2018) 553–574.
[15] M.Y. Wang, X. Wang, D. Guo, A level set method for structural topology optimization, Comput. Methods Appl. Mech. Eng. 192 (2003) 227–246.
[16] N.P. Van Dijk, K. Maute, M. Langelaar, F. Van Keulen, Level-set methods for structural topology optimization: A review, Struct. Multidiscip. Optim. (2013).
[17] O. Cansizoglu, O.L.A. Harrysson, H.A. West, D.R. Cormier, T. Mahale, Applications of structural optimization in direct metal fabrication, Rapid Prototyp. J. 14 (2008) 114–122.
[18] T.E. Müller, E. van der Klashorst, A quantitative comparison between size, shape, topology and simultaneous optimization for truss structures, Lat. Am. J. Solids Struct. 14 (2017) 2221–2242.
[19] N. Guo, M.C. Leu, Additive manufacturing: Technology, applications and research needs, Front. Mech. Eng. 8 (2013) 215–243.
[20] S. Bose, D. Ke, H. Sahasrabudhe, A. Bandyopadhyay, Additive manufacturing of biomaterials, Prog. Mater. Sci. (2018).
[21] T.D. Ngo, A. Kashani, G. Imbalzano, K.T.Q. Nguyen, D. Hui, Additive manufacturing (3D printing): A review of materials, methods, applications and challenges, Compos. Part B Eng. 143 (2018) 172–196.
[22] M. Javaid, A. Haleem, Additive manufacturing applications in medical cases: A literature based review, Alexandria J. Med. (2017).
[23] M.K. Thompson, G. Moroni, T. Vaneker, G. Fadel, R.I. Campbell, I. Gibson, A. Bernard, J. Schulz, P. Graf, B. Ahuja, F. Martina, Design for Additive Manufacturing: Trends, opportunities, considerations, and constraints, CIRP Ann. - Manuf. Technol. 65 (2016) 737–760.
[24] B. Vandenbroucke, J.P. Kruth, Selective laser melting of biocompatible metals for rapid manufacturing of medical parts, Rapid Prototyp. J. 13 (2007) 196–203.
[25] C. Körner, Additive manufacturing of metallic components by selective electron beam melting - A review, Int. Mater. Rev. 61 (2016) 361–377.
[26] X.P. Tan, Y.J. Tan, C.S.L. Chow, S.B. Tor, W.Y. Yeong, Metallic powder-bed based 3D printing of cellular scaffolds for orthopaedic implants: A state-of-the-art review on manufacturing, topological design, mechanical properties and biocompatibility, Mater. Sci. Eng. C. 76 (2017) 1328–1343.
[27] 3D SYSTEMS, Geomagic Freeform, (n.d.). https://www.3dsystems.com/software/geomagic-freeform (accessed September 21, 2018).
[28] J. Nedoma, Mathematical and Computational Methods and Algorithms in Biomechanics : Human Skeletal Systems, Wiley-Interscience, Hoboken, N.J., 2011.
[29] D.D. Lima, D.D. D'Lima, B.J. Fregly, S. Patil, N. Steklov, C.W. Colwell, Knee joint forces : prediction , measurement , and significance, Proc. Inst. Mech. Eng. H. 226 (2013) 95–102.
[30] B. Heinlein, I. Kutzner, F. Graichen, A. Bender, A. Rohlmann, A.M. Halder, A. Beier, G. Bergmann, ESB clinical biomechanics award 2008: Complete data of total knee replacement loading for level walking and stair climbing measured in vivo with a follow-up of 6-10 months, Clin. Biomech. 24 (2009) 315–326.
[31] D.E. Hurwitz, D.R. Sumner, T.P. Andriacchi, D.A. Sugar, Dynamic knee loads during gait predict proximal tibial bone distribution, J. Biomech. 31 (1998) 423–430.
[32] K. Murase, R.D. Crowninshield, D.R. Pedersen, T.S. Chang, An analysis of tibial component design in total knee arthroplasty, J. Biomech. 16 (1983) 13–22.
[33] D.A. Saravanos, P.J. Mraz, D.T. Davy, Shape Optimization of Tibial Prosthesis Components, Cleveland, 1993.
[34] K. Kaur, Stainless Steel and Titanium in Surgical Implants, (2013) 3. https://www.azom.com (accessed December 10, 2018).
[35] A.I. Bautista, A Finite Element Analysis of Tibial

Stem Geometry for Total Knee, California Polytechnic State University, 2015.
[36] LPW Carpenter Additive, Technical data sheet LPW 316L Stainless Steel, (2017) 1–2. https://www.lpwtechnology.com/.
[37] I. Kutzner, B. Heinlein, F. Graichen, A. Bender, A. Rohlmann, A. Halder, A. Beier, G. Bergmann, Loading of the knee joint during activities of daily living measured in vivo in five subjects, J. Biomech. 43 (2010) 2164–2173.
[38] J.B. Morrison, The mechanics of the knee joint in relation to normal walking, J. Biomech. 3 (1970) 51–61.
[39] C.M. Müller-Karger, C. Gonzál;lez, M.H. Aliabadi, M. Cerrolaza, Three dimensional BEM and FEM stress analysis of the human tibia under pathological conditions, C. - Comput. Model. Eng. Sci. 2 (2001) 1–13.
[40] R. Cazacu, L. Grama, Overview of Structural Topology Optimization Methods for Plane and Solid Structures, Ann. Univ. Oradea. (2014) 17–22.
[41] M.P. Bendsøe, N. Kikuchi, Generating optimal topologies in structural design using a homogenization method, Comput. Methods Appl. Mech. Eng. 71 (1988) 197–224.
[42] O. Sigmund, K. Maute, Topology optimization approaches: A comparative review, Struct. Multidiscip. Optim. (2013).
[43] M. Zhou, G.I.N. Rozvany, The COC algorithm, Part II: Topological, geometrical and generalized shape optimization, Comput. Methods Appl. Mech. Eng. 89 (1991) 309–336.
[44] Y. Di Li, B. Kuang, J. Liu, SIMP-Based Evolutionary Structural Optimization Method for Topology Optimization, Appl. Mech. Mater. 651–653 (2014) 2237–2240.
[45] D. Tcherniak, Topology optimization of resonating structures using SIMP method, Int. J. Numer. Methods Eng. 54 (2002) 1605–1622.
[46] T.Y. Chen, Y.H. Chiou, Structural Topology Optimization Using Genetic Algorithms, World Congr. Eng. 3 (2013) 3–7.
[47] D. Wang, S. Wu, Y. Yang, W. Dou, S. Deng, Z. Wang, S. Li, The effect of a scanning strategy on the residual stress of 316L steel parts fabricated by selective laser melting (SLM), Materials (Basel). 11 (2018) 1821.
[48] E. Segura-Cardenas, E. Ramirez-Cedillo, J. Sandoval-Robles, L. Ruiz-Huerta, A. Caballero-Ruiz, H. Siller, Permeability Study of Austenitic Stainless Steel Surfaces Produced by Selective Laser Melting, Metals (Basel). 7 (2017) 521.
[49] O. Zinger, K. Anselme, A. Denzer, P. Habersetzer, M. Wieland, J. Jeanfils, P. Hardouin, D. Landolt, Time-dependent morphology and adhesion of osteoblastic cells on titanium model surfaces featuring scale-resolved topography, Biomaterials. 25 (2004) 2695–2711.
[50] D. Mahmoud, M. Elbestawi, Lattice Structures and Functionally Graded Materials Applications in Additive Manufacturing of Orthopedic Implants: A Review, J. Manuf. Mater. Process. 1 (2017) 13.
[51] C. Beyer, D. Figueroa, Design and Analysis of Lattice Structures for Additive Manufacturing, J. Manuf. Sci. Eng. 138 (2016) 121014.